

Study of the Mg incorporation in CdTe for developing wide band gap Cd_{1-x}Mg_xTe thin films for possible use as top-cell absorber in a tandem solar cell

Omar S. Martínez^{a,b}, Aduljay Remolina Millán^a, L. Huerta^c, G. Santana^c, N.R. Mathews^a, M.L. Ramon-García^a, Erik R. Morales^a, X. Mathew^{a,*}

^a Centro de Investigación en Energía, Universidad Nacional Autónoma de México, 62580 Temixco, Morelos, México

^b Universidad Politécnica del Estado de Guerrero, Comunidad de Puente Campuzano, C.P. 40325 Taxco de Alarcón, Guerrero, México

^c Instituto de Investigaciones en Materiales, Universidad Nacional Autónoma de México. C.P 04510 México D.F., México

ARTICLE INFO

Article history:

Received 4 January 2011

Received in revised form 19 October 2011

Accepted 22 November 2011

Keywords:

Thin films

Evaporation

XPS

Semiconductivity

ABSTRACT

Thin films of Cd_{1-x}Mg_xTe with band gap in the range of 1.6–1.96 eV were deposited by vacuum co-evaporation of CdTe and Mg on glass substrates heated at 300 °C. Different experimental techniques such as XRD, UV–vis spectroscopy, SEM, and XPS were used to study the effect of Mg incorporation into the lattice of CdTe. The band gap of the films showed a clear tendency to increase as the Mg content in the film is increased. The Cd_{1-x}Mg_xTe films maintain all the structural characteristics of the CdTe, however, diminishing of intensity for the XRD patterns is observed due to both change in preferential orientation and change in atomic scattering due to the incorporation of Mg. SEM images showed significant evidences of morphological changes due to the presence of Mg. XRD, UV–vis spectroscopy, and XPS data confirmed the incorporation of Mg in the lattice of CdTe. The significant increase in band gap of CdTe due to incorporation of Mg suggests that the Cd_{1-x}Mg_xTe thin film is a candidate material to use as absorber layer in the top-cell of a tandem solar cell.

© 2011 Elsevier B.V. All rights reserved.

1. Introduction

In order to lower the cost per watt of the photovoltaic electricity, it is necessary to develop solar cells with high solar-to-electric conversion efficiency. Tandem solar cells promise high efficiencies by overcoming the limitations of the single junction solar cells. In this context development of promising materials for applications in tandem devices are interesting. A two junction all thin-film tandem solar cell with a top-cell absorber having band gap in the range 1.6–1.7 eV can attain efficiencies in the range of 25% [1]. Cd_{1-x}Mg_xTe is a candidate material for developing top-cell absorber layer with the above band gap criterion. The band gap of CdTe can be significantly opened by incorporating small amount of Mg, and the lattice mismatch between CdTe and MgTe is only little. Cd_{1-x}Mg_xTe thin films can be deposited by different techniques such as molecular beam epitaxy [2], sputtering [3,4], and co-evaporation [5,6]. Among these techniques co-evaporation is more economical, simple, and offers the flexibility of preparing thin films with different compositions by adjusting the evaporation rate of the individual source materials. There are recent reports about the development of Cd_{1-x}Mg_xTe thin films and the fabrication

of Cd_{1-x}Mg_xTe/CdS solar cells [4–6]. In this paper we are discussing the growth and a detailed characterization of Cd_{1-x}Mg_xTe thin films with $x=0-0.2$, developed by co-evaporation technique. Cd_{1-x}Mg_xTe thin films with $x>0.2$ can also be easily prepared by co-evaporation, however, for the application of this material as a top-cell absorber layer in tandem solar cells the required band gap is about 1.7 eV [1] which corresponds to $x<0.15$ [4,5]. The results discussed in this paper will enhance the knowledge about the material properties of Cd_{1-x}Mg_xTe thin film, and provide fundamental knowledge about this promising material.

2. Experimental details

Thin films of Cd_{1-x}Mg_xTe were deposited by co-evaporation on corning glass substrates of area 3 cm × 3 cm. The thickness of thin films was measured using a surface profiler, and it was in the range of 1.7 μm. The deposition of the films was performed at a base pressure of 5×10^{-6} Torr and at a substrate temperature of 300 °C. The film stoichiometry was controlled by adjusting the evaporation rate of CdTe and Mg independently. The conductivity type of the deposited films was determined to be p-type using the hot-probe technique. Structural characterization was performed with a Rigaku X-ray diffractometer with CuKα radiation and the optical transmittance spectra were recorded in the wavelength range of 500–900 nm using a Shimadzu UV–vis spectrophotometer. The

* Corresponding author.

E-mail address: xm@cie.unam.mx (X. Mathew).

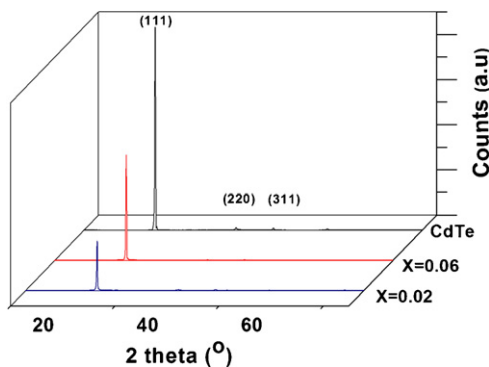


Fig. 1. XRD patterns of $\text{Cd}_{1-x}\text{Mg}_x\text{Te}$ thin films of identical thickness and deposited at same substrate temperature.

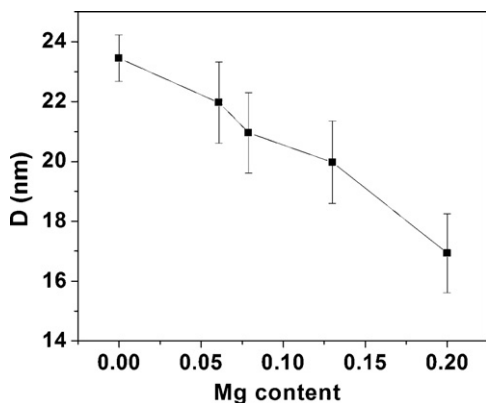


Fig. 2. The variation of the crystallite size with the Mg content (x) in the film.

morphological properties were investigated using a Hitachi scanning electron microscope FE SEM S-5500 and for the analysis of X-ray photoelectron spectroscopy (XPS) we used a system of ultra high vacuum (UHV) VG Microtech Multilab ESCA2000.

3. Results and discussion

The X-ray diffraction patterns of the $\text{Cd}_{1-x}\text{Mg}_x\text{Te}$ films and the reference CdTe film are shown in Fig. 1. To compare the structural properties of films with different amounts of Mg, films were made with the same thickness under the same deposition conditions. The diffractogram of CdTe ($x=0$) shows the planes (1 1 1), (2 2 0), (3 1 1)

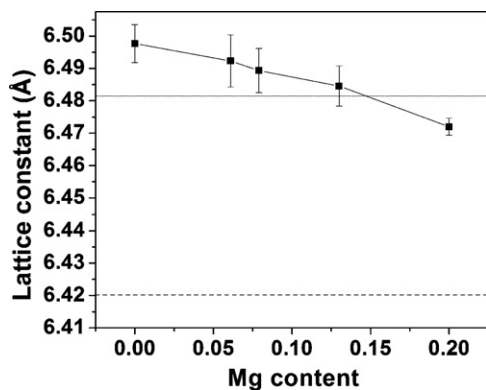


Fig. 3. Variation of lattice constant of $\text{Cd}_{1-x}\text{Mg}_x\text{Te}$ films with the amount of Mg incorporated in it. The markers are experimental data and the line is a guide to the eye. The dotted line corresponds to the stress free value of the lattice constant in the case of CdTe ($a_{\text{CdTe}} = 6.481 \text{ \AA}$) and dashed line corresponds to the stress free value of the lattice constant of CdMgTe ($a_{\text{MgTe}} = 6.420 \text{ \AA}$).

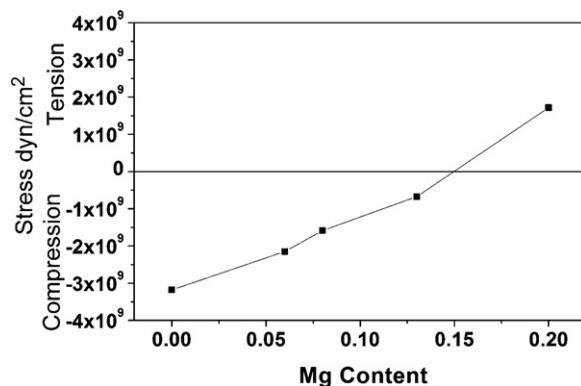


Fig. 4. The dependence of stress on the Mg content in $\text{Cd}_{1-x}\text{Mg}_x\text{Te}$ thin films.

conforming to the JCPDS card (15-0770), with a strong preference for the (1 1 1) plane. The CdTe film has cubic zinc blend lattice, the estimated value of the lattice parameter $a = 6.498 \text{ \AA}$. The diffractograms of $\text{Cd}_{1-x}\text{Mg}_x\text{Te}$ films with $x=0.06$ and $x=0.20$ are similar to that of CdTe indicating similar crystal structure of CdTe, and preferential growth for the plane (1 1 1), however, there is a significant decrease in the intensity of (1 1 1) reflection with increasing Mg content [5]. This decrease in intensity of the (1 1 1) reflection observed upon the incorporation of Mg in the lattice of CdTe can be either due to: (i) a change in preferential orientation grade for the film, (ii) change in X-ray scattering factor of the unit cell, or (iii) change in crystallite size. The preferential orientation grade of the films for the plane (1 1 1) was calculated using the XRD data and the orientation grade is found to decrease as the Mg content increased. The values of the preferential orientation grade was 1.84, 1.57, and 1.39, respectively, for $x=0$, 0.06, and 0.2. However, comparing the

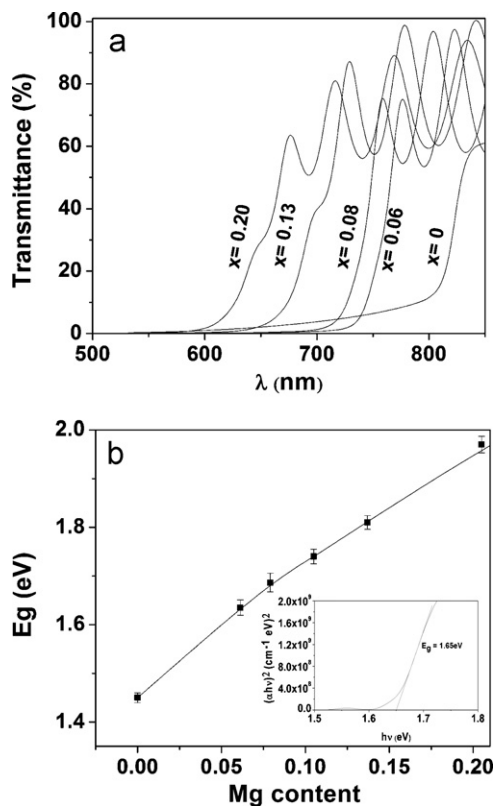


Fig. 5. (a) Transmittance spectra of $\text{Cd}_{1-x}\text{Mg}_x\text{Te}$ with $x=0$, 0.06, 0.08, 0.13, and 0.20 [5]. (b) Band gap vs. Mg content, inset is the Tauc plot of a typical $\text{Cd}_{1-x}\text{Mg}_x\text{Te}$ film with $x=0.065$, the corresponding band gap is 1.65 eV.

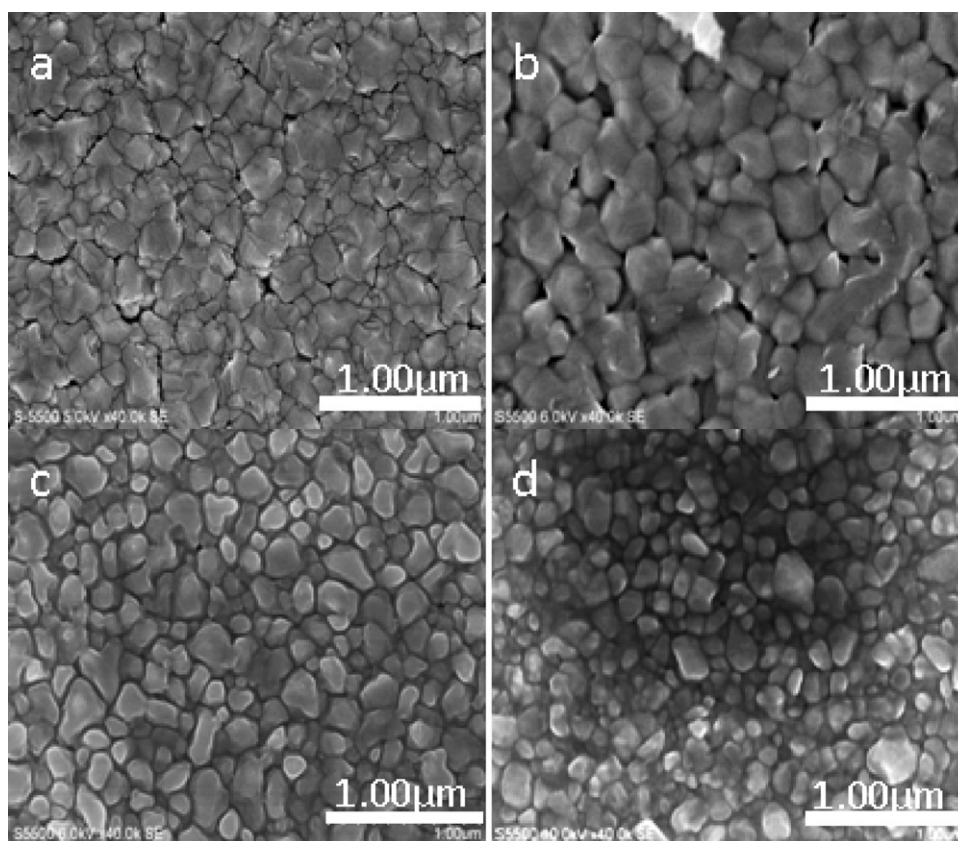


Fig. 6. SEM image of $\text{Cd}_{1-x}\text{Mg}_x\text{Te}$ films with different Mg contents. (a) $x=0$, (b) $x=0.06$, (c) $x=0.10$ and (d) $x=0.20$.

relative intensities of the XRD patterns of three films (Fig. 1), it can be concluded that the observed change in the XRD intensity is not only due to a change in the preferred growth but the atomic scattering factor is also playing a role [7]. The atomic scattering factor for Mg is only 9.8 \AA^{-1} , while that of Cd is 41.7 \AA^{-1} at $\theta = 11.85^\circ$ and for the X-ray wavelength $\lambda = 1.54 \text{ \AA}$.

The crystal size (D) was calculated using the FWHM of diffraction peak (1 1 1) and using the Scherer equation [8]. Fig. 2 shows the variation of the crystallite size with the amount of Mg in the film. In all these cases films with identical thickness were used, it is observed that with increasing the Mg content, the crystallite size decreases from 23 nm of the CdTe film to 17 nm for the $\text{Cd}_{1-x}\text{Mg}_x\text{Te}$ film with $x=0.20$. The calculated value of the lattice parameters of the $\text{Cd}_{1-x}\text{Mg}_x\text{Te}$ ($x=0-0.20$) is presented in Fig. 3. The lattice value of CdTe film $a = 6.498 \text{ \AA}$ is higher than the powder pattern (6.481 \AA) indicating that the deposited CdTe film is under stress. Fig. 4 shows

the relation between Mg content and the stress in the film. As can be seen from figure, with the increase in Mg content the stress changes from compressive to tensile. In the case of $\text{Cd}_{1-x}\text{Mg}_x\text{Te}$ films the lattice parameter is changed from 6.498 \AA to 6.47 \AA when x changed from 0 to 0.20, showing the effect of incorporation of Mg in the CdTe lattice. This nominal decrease in the lattice parameter is expected since the difference in lattice values of MgTe and CdTe is only 0.061 \AA . The lattice value for MgTe is 6.420 \AA [2,4] and that of CdTe is 6.481 \AA [9]. The observed decrease in lattice value of CdTe due to the incorporation of Mg is possible since Mg has the smallest ionic radius among the three elements Mg, Cd and Te. For example the ionic radii of Mg (+2), Cd (+2) and Te (-2) are 72, 95 and 221 pm, respectively, at a particular coordination number of 6 [10,11].

The transmittance spectra of the films recorded in the wavelength region 300–1000 nm were used to estimate the band gap of the films. The value of the absorption coefficient was estimated from the transmittance spectra (Fig. 5a). The band gap of the material was determined by plotting a graph with $(\alpha h\nu)^2$ vs. $h\nu$. The band gap showed a systematic change which is proportional to the amount of Mg incorporated in the film (Fig. 5b). Using the band gap values and Eq. (1), the Mg content (x) in the films can be estimated [2]:

$$E_g(x) = 1.5 + 0.3x(1 - x) + 2x \quad (1)$$

Fig. 6 shows the SEM images of $\text{Cd}_{1-x}\text{Mg}_x\text{Te}$ thin films with different Mg contents; these images show the impact of Mg incorporation on the morphology of the films, the changes in grain size and grain morphology are noticeable. Fig. 6a corresponds to the CdTe film ($x=0$), and the images b–d correspond to the $\text{Cd}_{1-x}\text{Mg}_x\text{Te}$ films with $x=0.06$, 0.13, and 0.20, respectively. The images a and b which corresponds to CdTe and $\text{Cd}_{0.94}\text{Mg}_{0.06}\text{Te}$ shows voids and large agglomerations of smaller grains, however, as the Mg

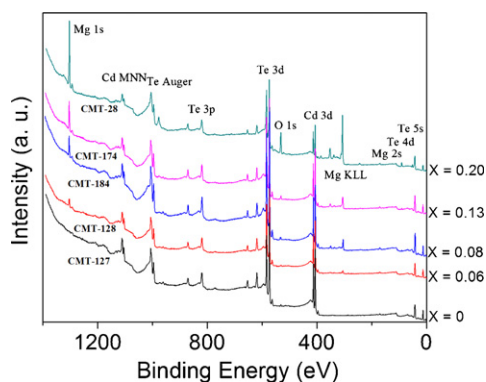


Fig. 7. XPS survey of $\text{Cd}_{1-x}\text{Mg}_x\text{Te}$ samples with $x=0$, 0.06, 0.08, 0.13, and 0.20.

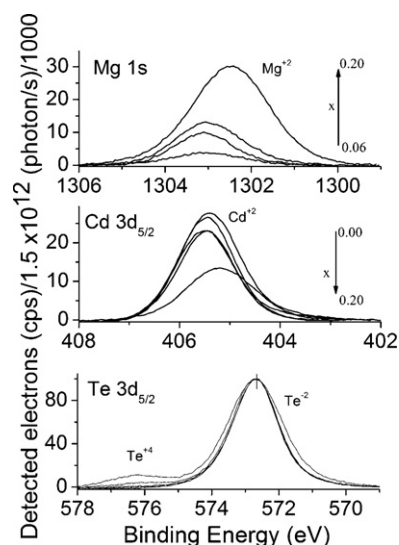


Fig. 8. High resolution XPS spectra of $\text{Cd}_{1-x}\text{Mg}_x\text{Te}$ in the region corresponds to the Mg 1s, Cd $3d_{5/2}$ and Te $3d_{5/2}$ core levels. The arrow indicates the increasing order of x values.

content increases the films become more compact with smaller grains. The average size of the grains are 213, 276, 213, and 156 nm for $\text{Cd}_{1-x}\text{Mg}_x\text{Te}$ films with $x = 0, 0.06, 0.13$ and 0.20 , respectively.

The XPS survey of the $\text{Cd}_{1-x}\text{Mg}_x\text{Te}$ films is shown in Fig. 7. The core level emissions corresponding to Mg 1s, Te $3d_{3/2}$, Te $3d_{5/2}$, Cd $3d_{3/2}$, Cd $3d_{5/2}$ and O 1s are clearly seen in the spectra. The O 1s peak can be due to the presence of traces of Te-O formed by the surface oxidation of Te. In addition, the Te $3p_{1/2}$, Te $3p_{3/2}$ and Te Auger peaks are also observed. The Mg 1s peak is observed with very low intensity in the case of $\text{Cd}_{1-x}\text{Mg}_x\text{Te}$ film with less amount of Mg ($x = 0.06$), and the intensity of the Mg 1s peak increased with the value of x indicating the effective incorporation of Mg in the CdTe lattice. Fig. 8 shows the high resolution spectra of XPS corresponding to binding energy (BE) of the core levels of Te $3d_{5/2}$, Cd $3d_{5/2}$ and Mg 1s for $x = 0.00, 0.06, 0.08, 0.13$ and 0.20 . The orbital Te $3d_{5/2}$ (572.70 eV) shows no chemical shift in BE with the addition of magnesium whereas the BE of Cd $3d_{5/2}$ shows a slight chemical shift which can be due to the incorporation of Mg. The corresponding values of the BE are 405.37, 405.49, 405.47, 405.46 and 405.19 eV, respectively, for $x = 0.00, 0.06, 0.08, 0.13$ and 0.20 . The Mg 1s orbital presents a chemical shift of 0.55 eV to the lower binding energy as the Mg content is increased to 0.20, this may be due to the fact that the charge transfer from Mg is lowered in the alloys with higher Mg content indicating that in these cases the charge state of Mg is less than Mg^{2+} [12].

4. Conclusions

The structural, morphological, and optical properties of $\text{Cd}_{1-x}\text{Mg}_x\text{Te}$ films ($x = 0, 0.06, 0.08, 0.13$ and 0.2) were investigated in detail to understand the incorporation of Mg in the lattice of CdTe. The band gap of the CdTe film increased with the amount Mg incorporated in the film. XRD analysis revealed that the $\text{Cd}_{1-x}\text{Mg}_x\text{Te}$ films maintain all the structural characteristics of the CdTe. SEM images showed noticeable evidences of morphological changes due to the incorporation of Mg. The XPS data confirmed the incorporation of Mg in the lattice of CdTe; the intensity of the Mg 1s peak showed a clear dependence on the amount of Mg in the film. Analysis of the binding energies of core levels Te $3d_{5/2}$, Cd $3d_{5/2}$ and Mg 1s showed that the binding energy of Te $3d_{5/2}$ was constant for the films with different amounts of Mg, however, Cd $3d_{5/2}$ and Mg 1s binding energies showed a dependence on the amount of Mg incorporated in the film, indicating the substitution of Cd by Mg.

Acknowledgements

This work at CIE-UNAM was partially supported by the projects CONACyT-PROINOVA 139562, SENER-CONACyT 117891, CONACyT 60762, ICyTDF, and PAPIIT IN 118409. A. Remolina acknowledges the postdoctoral scholarships received from ICyTDF and CLAF-Brazil. Authors acknowledge Gildardo Casarrubias Segura for technical support in SEM laboratory.

References

- [1] T.J. Coutts, J.S. Ward, D.L. Young, K.A. Emery, T.A. Gessert, R. Noufi, *Prog. Photovoltaics: Res. Appl.* 11 (2003) 359–375.
- [2] J.M. Hartman, J. Cibert, F. Kany, H. Mariette, M. Charleux, P. Alleysson, R. Langer, G. Feuillet, *J. Appl. Phys.* 80 (1996) 6257–6265.
- [3] S. Gupta, A.D. Compaan, *Appl. Phys. B* 95 (2009) 787–794.
- [4] X. Mathew, J. Drayton, V. Parikh, N.R. Mathews, X. Liu, A.D. Compaan, *Semicond. Sci. Technol.* 24 (2009) 015012.
- [5] O.S. Martínez, R.C. Palomera, J.S. Cruz, X. Mathew, *Phys. Status Solidi C* 6 (S1) (2009) S214–S218.
- [6] R. Dhere, K. Ramanathan, J. Scharf, H. Moutinho, B. To, A. Duda, R. Noufi, *Proceeding of IEEE 4th World Conference on Photovoltaic Energy Conversion*, 2006, doi:10.1109/WCPEC.2006.279513.
- [7] B.D. Cullity, *Elements of X ray diffraction*, Prentice Hall, 2001, pp. 634–635.
- [8] E. Lifshin, *X-Ray Characterization of Materials*, Wiley-VCH, New York, 1999, p. 37.
- [9] S. Lalitha, R. Sathyamoorthy, S. Senthilarasu, S. Subbarayan, *Sol. Energy Mater. Sol. Cells* 90 (2006) 694–703.
- [10] R.D. Shannon, C.T. Prewitt, *Acta Crystallogr.* B25 (1969) 925–945.
- [11] R.D. Shannon, *Acta Crystallogr.* A32 (1976) 751–767.
- [12] A. Talapatra, S.K. Bandyopadhyay, Pintu Sen, P. Barat, S. Mukherjee, M. Mukherjee, *Physica C* 419 (2005) 141–147.